Eksplorium
Volume 46 No. 2, November 2025: 93–108

p-ISSN 0854-1418
e-ISSN 2503-426X

Analysis of Rock Mass Quality and Support Requirements Using Q-System – Case Study: Kalan Uranium Exploration Tunnel, West Kalimantan, Indonesia

Wira Cakrabuana[1]*, Indra A. Dinata[2], Yuni Faizah[3], Dhatu Kamajati[4], Putri Rahmawati[4]
[1]Research Center for Geological Hazards, Research Organization for Earth Sciences and Maritime, National Research and Innovation Agency (BRIN), Serpong Main Rd., Tangerang Selatan 15324, Indonesia
[2]Geological Engineering Study Program, Institut Teknologi Bandung (ITB), Ganesa St., No. 10, Bandung 40132, Indonesia
[3]Directorate of Research and Innovation Utilization in Industry, National Research and Innovation Agency (BRIN), M. H. Thamrin St., No. 8, Jakarta Pusat 10340, Indonesia
[4]Bureau of Public, General, and Secretarial Communication, National Research and Innovation Agency (BRIN), M. H. Thamrin St., No. 8, Jakarta Pusat 10340, Indonesia
*E-mail: wira006@brin.go.id

Article received: 27 October 2025, revised: 25 November 2025, accepted: 30 November 2025
DOI: 10.55981/eksplorium.2025.13575

ABSTRACT

The Kalan uranium exploration tunnel was one of the nuclear minerals research facilities in Indonesia. This 618 m long tunnel, located in West Kalimantan, Indonesia, was built on Eko Remaja Hill and operated from 1980-2021. In this tunnel, uranium mineralization occurs as irregular veins (stockworks) in metasiltstone and metapelite. The high density of these veins causes the formation of several weak zones in the tunnel. These weak zones cause rock and soil failures at several locations in the tunnel. The study aims to evaluate the quality of the rock mass surrounding the tunnel and determine the support requirements necessary to prevent further structural failures. Scanline surveys were carried out in several zones that have not experienced failures to obtain Q-system parameters. Based on the results of the analysis, the rock mass that makes up the Kalan tunnel has a Q value of 0.61–48.22, so that it belongs to the class of very poor-very good rocks. By plotting the Q value with its equivalent dimension (ED) on the rock support chart, it is estimated that the support required by the tunnel is average bolt spacing without fiber-reinforced sprayed concrete. The ultimate pressures of the roof and wall support can bear are 0.04–0.24 MPa and 0.03–0.17 MPa, respectively.

Keywords: rock mass quality, support requirements, Q-system, Kalan tunnel

INTRODUCTION

The Kalan (or Eko Remaja) uranium exploration tunnel, located in West Kalimantan, was one of the research facilities for nuclear minerals (especially uranium) in Indonesia [1]–[5]. This tunnel was constructed on Eko Remaja Hill in 1980. In addition, research, exploration, and mining activities were conducted at this facility until they began to scale back in 1991. The tunnel was closed permanently in 2021.

Until 2019, there have been several rock and soil failures inside the Kalan tunnel (Table 1) [4], [6], [7]. Rocks mostly failed in a wedge-type, while soils failed in a circular-type. Wooden poles installed in several weak zones are no longer considered capable of supporting the tunnel safely. A comprehensive review of the surrounding rock mass is required to assess the tunnel's stability.

This study aims to assess the rock mass quality in the Kalan tunnel and to determine

the support needed to prevent further failures. The Q-System utilization in uranium-bearing rocks is still limited [8], [9], so the study done in this article can be considered novel, especially in Indonesia. The Q-System was selected for this study as it is a globally recognized rock mass classification method, widely considered the most appropriate for assessing tunnel stability [10]–[12].

Table 1. The record of failure events at Kalan tunnel [4], [6], [7]

No.	Year of event	Tunnel depth (m)
1	2009	314.25
2	2011	568
3	2011	598
4	2011	603
5	2014	560.68
6	2015	568.50
7	2019	600

The methods used in this study are the scanline survey and Q-system rock mass classification. The scanline survey aims to record the physical properties of rock masses (in this case, metasedimentary rocks) and discontinuities (in this case, stockworks and other geological structures) that make up the tunnel body [13]–[17]. Based on these parameters, the quality of rock mass will be ranked through the Q-system rock mass classification [18]. A Q value that reflects the quality of the rock mass, combined with the tunnel's equivalent dimension (ED), can be used to determine the type of support needed by the tunnel [19].

RESEARCH LOCATION

The Kalan tunnel is located in Kalan Village, Ella Hilir District, Melawi Regency, West Kalimantan Province, Indonesia. The Kalan area is located in the upper Kalan River valley, situated on the left branch of the Ella Hilir River, which eventually flows into the Melawi River. The location of the study area is shown in Figure 1.

The Kalan tunnel was built through Eko Remaja Hill with entrances on both sides, namely Remaja entrance and TRK-7 entrance [1], [2]. The tunnel is located at an elevation of 450 m above sea level, has a length of 618 m, and is directed N 50° E [7], [20]–[22]. The Kalan tunnel has three zones that have been installed with wooden supports, namely at meters 0–50, meters 297–355, and meters 538–618 [4], [23]. A schematic illustration of the tunnel can be seen in Figure 2 (modified from [4]).

The regional geology of the Kalan area and its surroundings is composed of the Pinoh metamorphic rocks, Sepauk tonalites, and Sukadana granites [24]–[28]. The Pinoh metamorphic rocks date to the Carboniferous-Triassic age and are composed of quartz-muscovite schist, phyllite, slate, hornfels, some meta-tuffs, and quartzite. These rocks locally contain andalusite, cordierite, and biotite, with rare sillimanite and garnet. The Pinoh metamorphic rock was intruded by Sepauk tonalites and was then intruded again by Sukadana granites [23], [29]–[31].

The Kalan tunnel is in the lower series type of volcano-sedimentary rocks group, which is part of the Pinoh metamorphic rocks [25], [29], [30], [32]–[34]. This group is composed of an intercalation between metasiltstone and metapelite containing biotite, andalusite, cordierite, and rhyodacite interbedding. The detailed geological map of the Kalan tunnel is pictured in Figure 3.

p-ISSN 0854-1418
e-ISSN 2503-426X

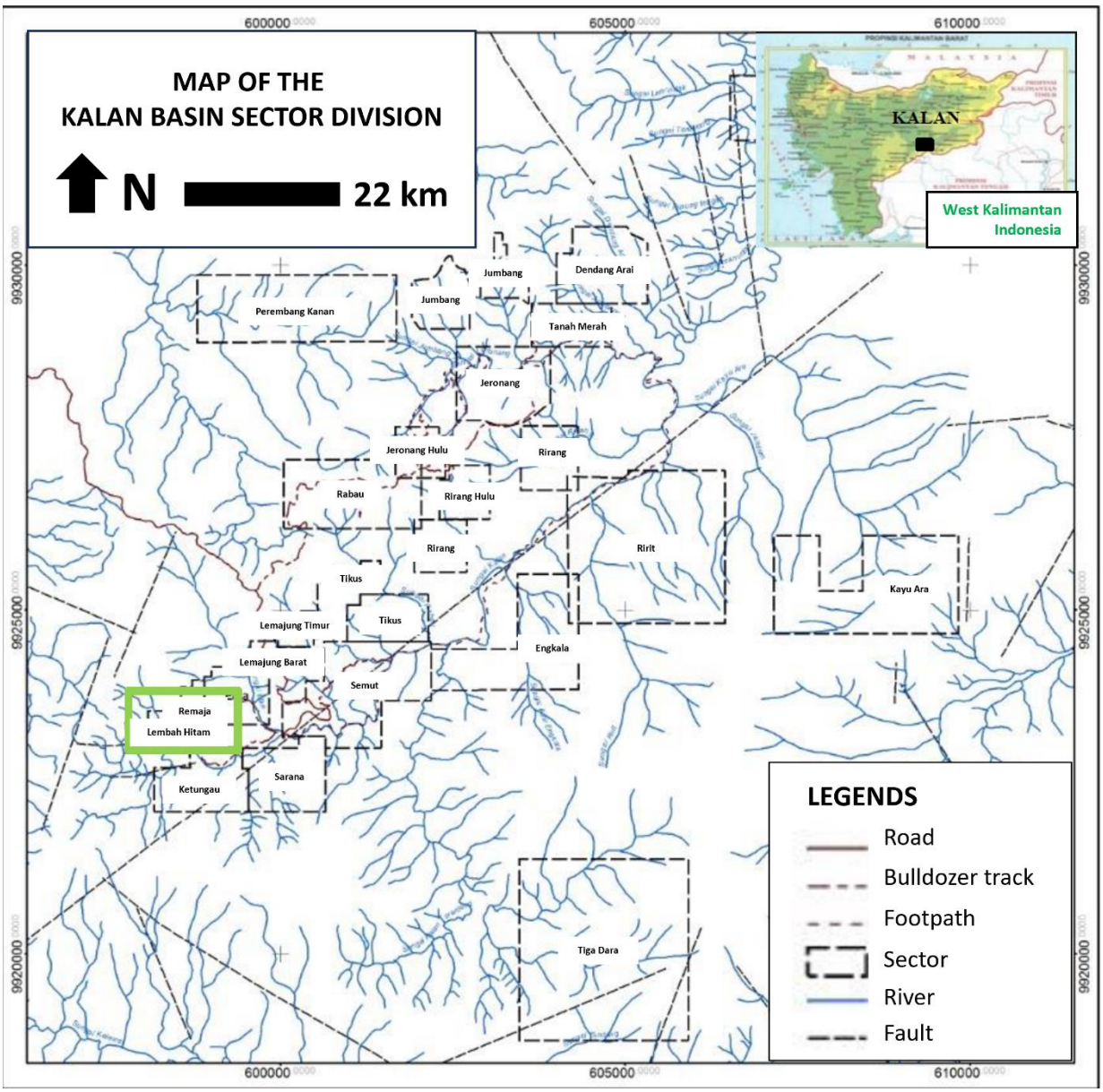

Figure 1. Map of the Kalan basin sector division; the green square marks the study location (modified from [2])

The geological structures in Kalan and its surroundings are formed through two stages of deformation, plastic deformation and brittle deformation [2], [22], [30], [31], [35]–[38]. Plastic deformation initiated with folding and progressed to the development of schistosity within the Triassic rocks. The fold is in the direction of N 70° E, while the schistosity is in the direction of 70° to the north relative to the fold axis. Initial brittle deformation during the Cretaceous period created fractures parallel to the schistosity; these were subsequently mineralized with uranium, resulting in the formation of stockworks. The second brittle deformation formed another stockworks containing calcite and gypsum that cut the stockworks resulting from the first brittle deformation.

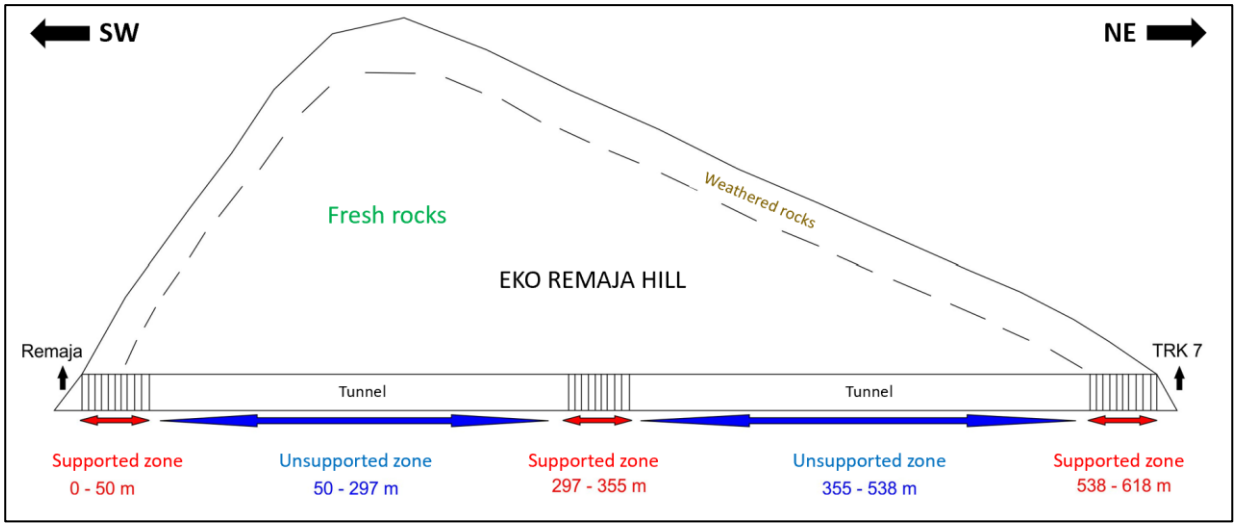

Figure 2. The schematic illustration of the Kalan tunnel (modified from [4])

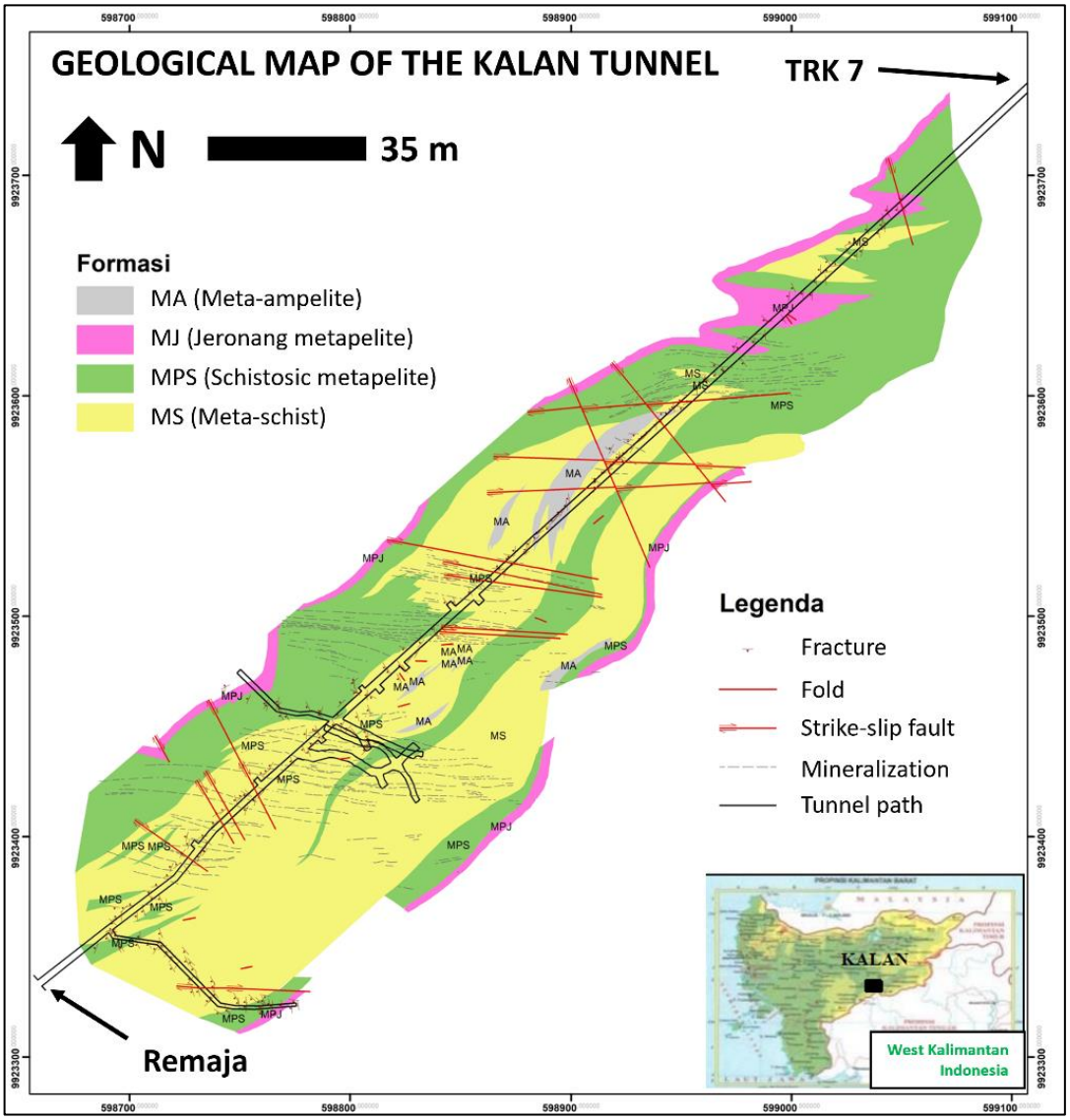

Figure 3. The geological map of the Kalan tunnel (modified from [20])

p-ISSN 0854-1418
e-ISSN 2503-426X

DATA AND METHODS

The scanline data used in this paper are obtained from the previous study [4]. Scanline surveys were conducted along the sections of the tunnel where wooden supports had not been installed, specifically between distances 50–297 m and 355–538 m. The scanline survey is carried out by stretching the tape on a segment of the rock outcrop, then recording the physical properties of the rock mass and discontinuity along the segment passed by the tape [13]–[17]. A schematic illustration of the scanline survey can be seen in Figure 4 [39].

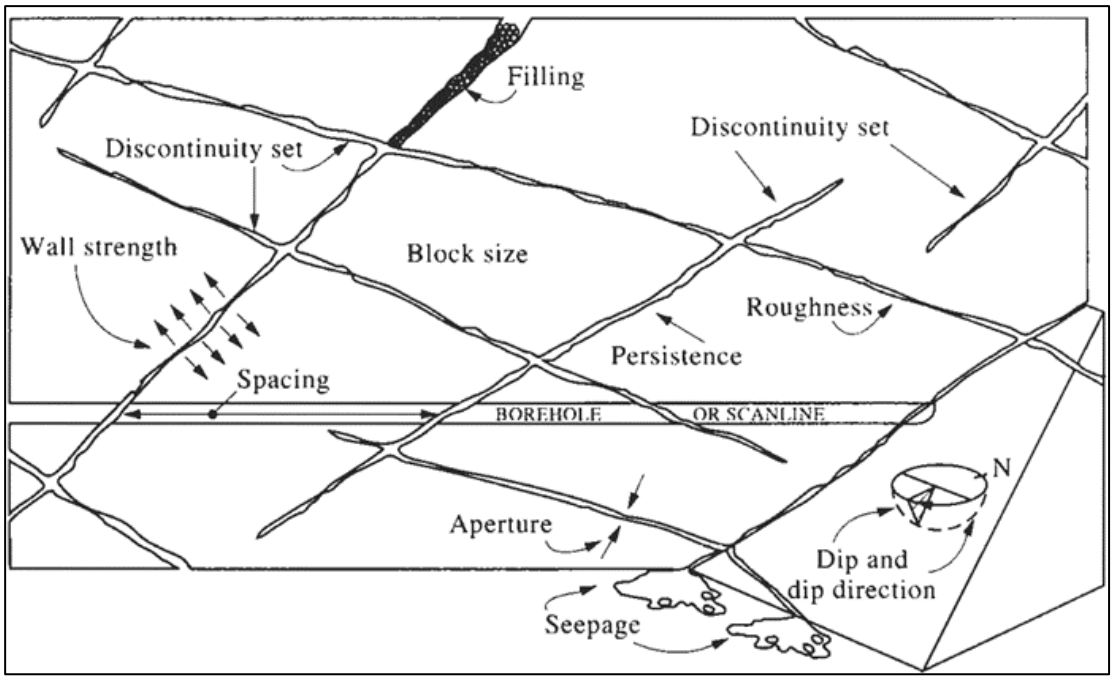

Figure 4. The illustration of discontinuity properties on the rock mass recorded in a scanline survey [39]

The physical properties of the rock mass recorded include color, grain size, type, structure, block size, and degree of weathering [13]–[15]. The recorded physical properties of the discontinuities include type, dip, dip direction, persistence, aperture, infill type and strength, surface roughness, groundwater conditions, and spacing. Both properties will be used as materials to rank the quality of rock masses with the Q-system [18].

The Q-system is a rock mass classification developed at the Norwegian Geotechnical Institute (NGI) in 1971–1974 [18]. This classification is intended to assess the stability of underground openings. Based on the estimate of six parameters, a Q value can be obtained. The Q value describes the quality of the rock mass that makes up the underground opening. The Q value, together with the opening's equivalent dimension (ED), can indicate what type of support is needed to maintain the stability of the underground opening. The Q-System was developed based on empirical cases involving jointed rock masses and weak zones; therefore, it is a highly appropriate classification method for the conditions found in this study. There are 1260 case records to prove the efficacy of this approach; it is the best classification system for tunnel supports [12], [40]–[42]. The Q value is calculated using a formula as listed in Equation 1 as follows:

$$Q = \frac{RQD}{J_n}\frac{J_r}{J_a}\frac{J_w}{SRF} \quad (1)$$

where:
Q : Q value
RQD : Rock quality designation (%)
J_n : Joint set number
J_r : Joint roughness number
J_a : Joint alteration number
J_w : Joint water reduction factor
SRF : Stress reduction factor

RQD was introduced to classify the rock mass quality simply [43]. In this study, RQD was empirically determined through Equation 2 as follows [44]:

$$RQD = 100(0.1\lambda + 1)e^{-0.1\lambda} \quad (2)$$

where:
RQD : Rock quality designation (%)
λ : Discontinuity frequency (/m)

J_n is a value to express the number of discontinuity sets that exist in a rock mass [18]. J_r is a value that reflects the surface shape of a joint wall [45]. J_a is a value depicting how far an alteration occurs in the rock mass. J_w is a value describing the influence of water on the joint wall.

In general, SRF describes the relation between stress and rock strength around an underground opening [45]. SRF can then be calculated from the relation between the rock uniaxial compressive strength (σ_c) and the major principal stress (σ_1) or the relation between maximum tangential stress (σ_θ) and σ_c in massive rock. Since no in-situ stress measurements have yet been conducted at the tunnel, an empirical approach and expert judgement are utilized to determine the SRF.

It was mentioned before that the Q value can be used to evaluate the support design. In addition to the Q value, two other factors are decisive for the support design in underground openings and caverns. These factors are the dimensions (i.e., span or height of the underground opening) and the safety requirements. Generally, there will be an increasing need for support with increasing span and wall height. Safety requirements will depend on the purpose of the excavation (i.e., a road tunnel or underground power house will need a higher level of safety than a water tunnel or a temporary excavation in a mine). To express safety requirements, a factor called the excavation support ratio (ESR) is used [46].

A low ESR value reflects a requirement for more stringent safety standards and robust support, whereas higher ESR values indicate that a lower density of reinforcement is acceptable. The classification of ESR is listed in Table 2 [46]. In addition to span or wall height and ESR, there is an "equivalent dimension" formulated as in Equation 3.

$$\frac{Span\ or\ height\ in\ m}{ESR} = Equivalent\ dimension \quad (3)$$

Table 2. ESR values [46]

	Type of excavation	ESR
A	Temporary mine openings, etc.	2–5
B	Permanent mine openings, water tunnels for hydro power (excluding high-pressure penstocks), pilot tunnels, drifts and headings for large openings, surge chambers	1.6–2.0
C	Storage caverns, water treatment plants, minor road and railway tunnels, and access tunnels	1.2–1.3
D	Power stations, major roads, and railway tunnels, civil defense chambers, portals, and intersections	0.9–1.1
E	Underground nuclear power stations, railway stations, sports and public facilities, factories, and major gas pipeline tunnels	0.5–0.8

The calculated Q value and the ED will determine the requirements for permanent support design. In the rock support chart [47],

p-ISSN 0854-1418
e-ISSN 2503-426X

the Q values are plotted along the horizontal axis and the equivalent dimension along the vertical axis on the left-hand side. The support chart gives an average of the empirical data from examined cases. The chart does not use rigid support classes; instead, it provides a continuous scale for determining both bolts spacing and the thickness of sprayed concrete. Not only the type of support, but the chart also indicates the energy absorption of the fiber-reinforced sprayed concrete, as well as the bolt length and design of reinforced ribs of sprayed concrete.

RESULTS AND DISCUSSION

Using scanline data in the form of discontinuity spacing, RQD calculations are performed using Equation 2. The calculation yielded an RQD value with a range of 72.61–97.53% which means that the rock mass that makes up the tunnel has fair to excellent quality. The sample of the RQD calculation result is listed in Table 3.

Using scanline data in the form of discontinuity positions, plotting was carried out on stereonets and rosette diagrams. The results showed that there were four clusters of J_n values in the discontinuity in the tunnel, namely J_n = 2 (one joint set), J_n = 3 (one joint set plus random), J_n = 4 (two joint sets), and J_n = 6 (two joint sets plus random). The sample of each J_n cluster is pictured in Figure 5.

Table 3. The sample of RQD calculation

No.	Station	Number of discontinuities	Length of scanline	Frequency of discontinuity	RQD (%)	Description
1	50–55 m	12	5	2.40	97.53	Excellent
2	55–60 m	12	5	2.40	97.53	Excellent
3	60–65 m	22	5	4.40	92.72	Excellent
4	65–72 m	29	7	4.14	93.43	Excellent
5	75–80 m	50	7	7.14	83.88	Good
6	80–85 m	38	5	7.60	82.27	Good
7	85–90 m	40	5	8.00	80.84	Good
8	90–95 m	40	5	8.00	80.84	Good
9	95–100 m	33	5	6.60	85.76	Good
10	100–105 m	42	5	8.40	79.39	Good

Using scanline data in the form of a description of surface roughness and shape, a J_r value was categorized for the discontinuity surface in the tunnel. As a result, there are four clusters of J_r values, namely J_r = 1 (smooth, planar), J_r = 1.5 (rough, irregular, planar), J_r = 2 (smooth, undulating), and J_r = 3 (rough or irregular, undulating). The sample of some J_r description result is listed in Table 4.

Based on scanline data in the type and strength of infilling, the J_a was determined to characterize the degree of discontinuity alteration within the tunnel. As a result, there are two groups of J_a values, namely J_a = 0.75 (tightly healed, hard, non-softening, impermeable filling) and J_a = 1 (unaltered joint walls, surface staining only). The sample of some J_a description result is listed in Table 5.

Using scanline data in the form of a description of groundwater conditions, a categorization of J_w values for discontinuity in the tunnel are calculated. As a result, all discontinuities are in the category of J_w = 1 (dry excavation or minor flow).

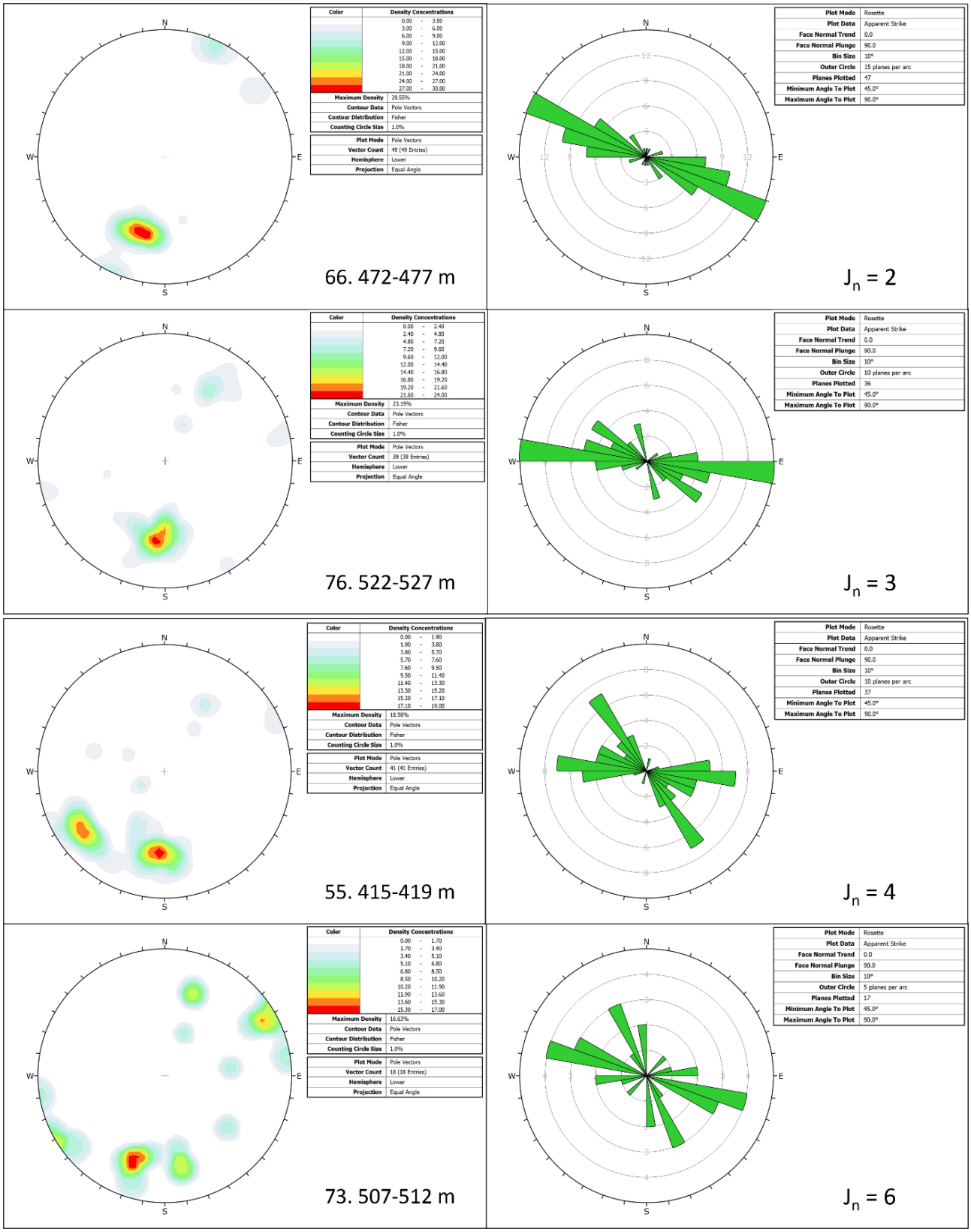

Figure 5. The sample of each J_n cluster

p-ISSN 0854-1418
e-ISSN 2503-426X

Table 4. The sample of each J_r description

No.	Station	Description	J_r
19	145–150 m	Smooth, planar	1
34	240–245 m	Rough, irregular, planar	1.5
41	282–287 m	Smooth, undulating	2
57	427–432 m	Rough or irregular, undulating	3

Table 5. The sample of each J_a description

No.	Station	Description	J_a
41	282–287 m	Unaltered joint walls, surface staining only	1
43	292–297 m	Tightly healed, hard, non-softening, impermeable filling	0.75

The determination of SRF values in this study involves the most assumptions because stress measurements have never been carried out at the location of this study. The calculation of the SRF value is carried out with the help of *RocLab* software, which is one of *Rocscience's* products [48]. Plotting the value of minimum stress (σ_3) on the x-axis and the value of maximum stress (σ_1) on the y-axis was carried out. Plotting was carried out with the Hoek-Brown failure criteria [49]. Inputs entered to create the plot include the compressive strength of the intact rock (σ_{ci}), the Geological Strength Index (GSI), the Hoek-Brown constant for the intact rock (m_i), and the disturbance factor (D).

The compressive strength of the intact rock (σ_{ci}) is obtained from the conversion of the rock hardness measurement using the Schmidt hammer by Equation 4 as follows [50]:

$$\sigma_{UCS} = 0.33(R_L \rho)^{1.35} \quad (4)$$

where:

σ_{UCS} : Uniaxial compressive strength (UCS) (MPa)
R_L : L-type Schmidt hammer rebound value
ρ : Natural density (g/cm^3)

The Geological Strength Index (GSI) is obtained empirically through Equation 5, as follows [51]:

$$GSI = 1.5\, JCond_{89} + RQD/2 \quad (5)$$

where:

GSI : Geological strength index
$JCond_{89}$: Joint condition rating of the RMR_{89}
RQD : Rock quality designation (%)

The Hoek-Brown constant for intact rocks (m_i) is empirically obtained through an estimation of m_i values by rock type [52]. The rocks in this study were fine-grained metasedimentary rocks, so the closest type of rock was slates (m_i = 7±4). The disturbance factor (D) is obtained through the estimation table of the D value based on the degree of disturbance experienced by the rock mass [49], [53]. The D value used in this study was 0.8, with the description "very poor-quality blasting in a hard rock tunnel results in severe local damage, extending 2 or 3 m, in the surrounding rock mass". In addition to these four parameters, for the application of tunnels, *RocLab* requires the input of unit weight and tunnel depth. The unit weight and tunnel depth input were 0.027 MN/m^3 and 618 m, respectively [54]. Figure 6 is an example of a screenshot showing the plot results in the *RocLab* software.

In some geotechnical practice, the major principal stress value (σ_1) used to determine the SRF value is usually obtained from the intersection between the Hoek-Brown failure criteria curve (red line) and the Mohr-Coulomb (blue line) [48]. In Figure 6, there are two intersection points; the upper intersection point with a higher value, σ_1, was picked for the SRF calculation. A higher σ_1 value results in a higher SRF value, so the resulting Q value is lower (pessimistic or conservative). Some

examples of SRF calculation results are listed in Table 6.

Using the six parameters obtained previously, the Q value was calculated according to Equation 1 (Table 7). The Q value of the rock mass that makes up the Kalan tunnel ranges from 0.61–48.22 (very poor-very good) with the following details:

- Very poor category (0.1 <Q ≤1) by 3.85%;
- Poor category (1 < Q ≤ 4) by 14.10%;
- Fair category (4 < Q ≤ 10) by 26.92%;
- Good category (10 < Q ≤ 40) by 53.85%; and
- Very good category (40 < Q ≤ 100) by 1.28%.

Next, the calculation of the Equivalent Dimension (ED) was carried out using Equation 3. For roof support, span is used, while for the wall support, wall height is used. The ED value is required to plot on the rock support chart. As a result, the ED value for roof support was 0.67, while four groups of ED values for wall support were obtained, namely 1.67 (by 85.90%), 1.87 (by 3.85%), 2.00 (by 7.69%), and 2.67 (by 2.56%). Because the minimum ED value listed on the chart is 1, the ED value of 0.67 was assumed to be 1. For the wall support, the Q values must be adjusted as in Table 8 [18].

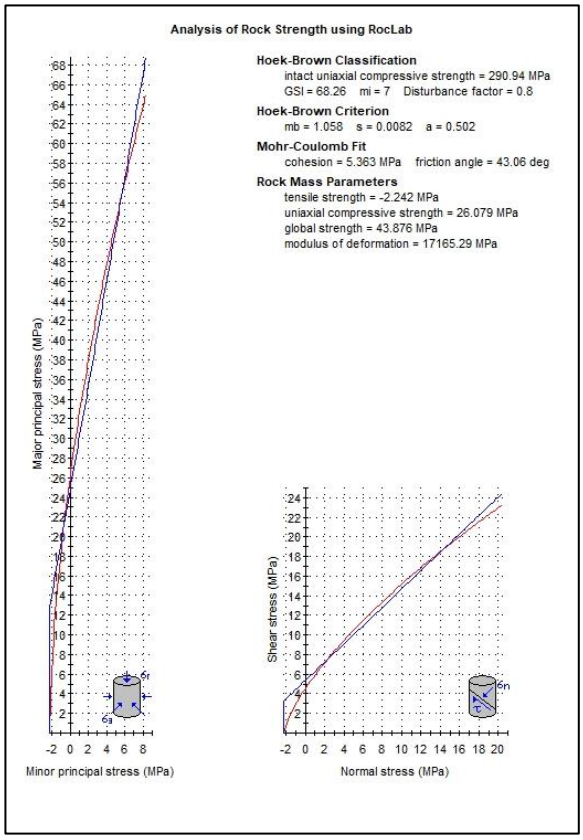

Figure 6. The sample of the *RocLab* plot result for Station 1 (50–55 m); the red line represents the Hoek-Brown failure criteria, while the blue one represents the Mohr-Coulomb failure criteria

Table 6. The sample of the SRF calculation

No.	Station	σ_{ci} (MPa)	Upper intersection σ_1 (MPa)	Lower intersection σ_1 (MPa)	Upper σ_{ci}/σ_1	Lower σ_{ci}/σ_1	Upper SRF	Lower SRF
1	50–55 m	290.94	55	22	5.3	13.2	5	1
14	120–125 m	290.94	35	13.5	8.3	21.6	3.5	1
25	186–191 m	290.94	29.5	11.5	9.9	25.3	27.5	1
40	277–282 m	290.94	51.5	19.5	5.6	14.9	50	2

Fourteen representative points, picked from various rock mass quality classes and ED values, were plotted on the chart (Table 9 and Figure 7). Both the roof and wall support cases and all points were in Zone 1, meaning that the support needed by the tunnel is average space bolting without fiber-reinforced sprayed concrete. It should be clarified that being in Zone 1 does not mean the rock mass is inherently "good"; under given tunnel geometry and ESR, the average bolting is sufficient. The unsupported zones of the Kalan

p-ISSN 0854-1418
e-ISSN 2503-426X

tunnel are in a safe condition and do not need any significant reinforcement.

The previous study concludes that the tunnel is comprised of fair-good rocks (RMR 52–71) and needs two kinds of support with specific size (3–4 m-long rock bolt with 1.5–2.5 space and 50–100 mm-thick conventional shotcrete) [4]. Compared to the previous study, this paper suggests a wider range of rock mass quality categories and a more optimistic estimate of the support requirement.

Besides the support requirements, the ultimate support pressures could also be calculated. The support pressures for both the roof and wall can be determined using Equations 6–7 [18] as follows:

$$p_v = \frac{0.2{J_n}^{1/2}}{3J_r} Q^{-1/3} \quad (6)$$

$$p_h = \frac{0.2{J_n}^{1/2}}{3J_r} {Q_w}^{-1/3} \quad (7)$$

where:

p_v : Ultimate roof support pressure (MPa)
p_h : Ultimate wall support pressure (MPa)
J_n : Joint set number
J_r : Joint roughness number
Q : Actual Q values
Q_w : Adjusted Q values

Table 10 lists the support pressure calculation results of the 14 sample points. The results indicate that the ultimate pressure capacity of the roof support ranges from 0.04 to 0.24 MPa, while the capacity for the walls ranges from 0.03 to 0.17 MPa.

This study serves as a preliminary step toward a comprehensive safety assessment of the Kalan tunnel, particularly regarding its potential reactivation for nuclear mineral exploration and exploitation. This paper still contains some limitations on its data and methods. The assessment can be further refined by incorporating primary data, such as rock strength and in-situ stress measurements, and utilizing advanced analytical techniques like numerical modeling.

Table 7. Some samples of the Q value calculation

No.	Station	RQD (%)	J_n	J_r	J_a	J_w	SRF	Q value	Quality description
78	532–538 m	80.84	4	1.5	1	1	50	0.61	Very poor
34	240–245 m	91.55	3	1.5	0.75	1	50	1.22	Poor
75	517–522 m	80.12	3	1	1	1	5	5.34	Fair
54	410–415 m	76.47	3	2	1	1	5	10.20	Good
14	120–125 m	84.38	2	3	0.75	1	3.5	48.22	Very good

Table 8. Conversion from actual Q values to adjusted Q values for the design of wall support [18]

Rock mass quality	Q values	Wall factor (Q_w)
Good	>10	5Q
Intermediate	0.1–10	2.5Q
Poor	<0.1	Q

Table 9. The sample points to plot on the rock support chart

No.	Station	Span (m)	Wall height (m)	ESR	ED (roof support)	ED (wall support)	Q	Q_w
78	532–538 m	2	5	3	0.67	1.67	0.61	1.53
34	240–245 m	2	5	3	0.67	1.67	1.22	3.05
67	477–482 m	2	5	3	0.67	1.67	3.86	9.65
75	517–522 m	2	5	3	0.67	1.67	5.34	13.35
70	492–497 m	2	5	3	0.67	1.67	10.00	25.00
54	410–415 m	2	5	3	0.67	1.67	10.20	51.00
5	75–80 m	2	6	3	0.67	2.00	14.91	74.55
9	95–100 m	2	5.6	3	0.67	1.87	17.15	85.75
7	85–90 m	2	5.6	3	0.67	1.87	21.56	107.80
12	110–115 m	2	8	3	0.67	2.67	22.13	110.65
15	125–130 m	2	6	3	0.67	2.00	32.34	161.70
13	115–120 m	2	8	3	0.67	2.67	33.05	165.25
17	135–140 m	2	5	3	0.67	1.67	33.47	167.35
14	120–125 m	2	5	3	0.67	1.67	48.22	241.10

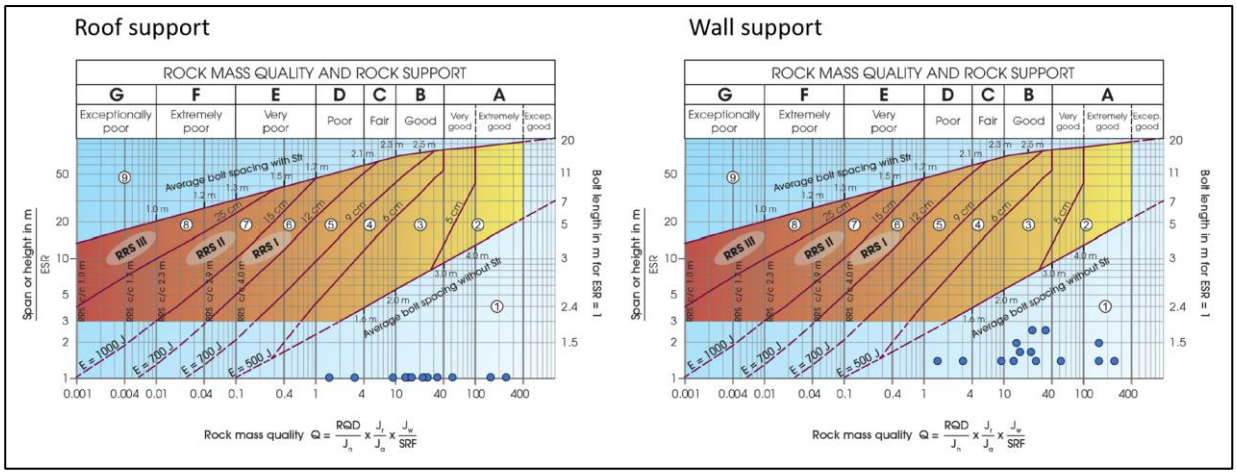

Figure 7. The plotting results on the rock support chart [47]; the blue dots represent the sample points

Table 10. Calculated support pressure values for specific sample points

No.	Station	J_n	J_r	Q	Q_w	p_v (MPa)	p_h (MPa)
78	532–538 m	4	1.5	0.61	1.53	0.24	0.17
34	240–245 m	3	1.5	1.22	3.05	0.16	0.12
67	477–482 m	6	1.5	3.86	9.65	0.16	0.12
75	517–522 m	3	1	5.34	13.35	0.07	0.05
70	492–497 m	2	1	10.00	25.00	0.04	0.03
54	410–415 m	3	2	10.20	51.00	0.11	0.06
5	75–80 m	3	2	14.91	74.55	0.09	0.05
9	95–100 m	2	2	17.15	85.75	0.07	0.04
7	85–90 m	2	2	21.56	107.80	0.07	0.04
12	110–115 m	3	3	22.13	110.65	0.12	0.07
15	125–130 m	2	3	32.34	161.70	0.09	0.05
13	115–120 m	2	3	33.05	165.25	0.09	0.05
17	135–140 m	2	3	33.47	167.35	0.09	0.05
14	120–125 m	2	3	48.22	241.10	0.08	0.05

p-ISSN 0854-1418
e-ISSN 2503-426X

CONCLUSION

The rock mass surrounding the Kalan tunnel ranges in quality from 'very poor' to 'very good,' with a Q value between 0.61 and 48.22. Notably, 53.85% of the assessed rock mass is classified as 'good' ($10 < Q \leq 40$). By plotting the Q values together with the ED values on the rock support chart, it is known that the support requirement for both the roof and wall of the tunnel is average space bolting without fiber-reinforced sprayed concrete. The allowable ultimate pressures for roof and wall supports are 0.04–0.24 MPa and 0.03–0.17 MPa, respectively.

ACKNOWLEDGMENT

Thank you to the managers and researchers in the former Center for Nuclear Minerals Technology, Badan Tenaga Nuklir Nasional, who have supported the entire process of this research.

REFERENCES

[1] A. Zaenal, "Beton Cetak Bertulang sebagai Alternatif Pengganti Kayu Penyangga di Terowongan Eksplorasi U Eko Remaja Kalimantan Barat," in *Prosiding Seminar Geologi Nuklir dan Sumberdaya Tambang*, 2006.

[2] D. Kamajati, H. Syaeful, and B. G. Mirna, "Evaluasi Massa Batuan Terowongan Eksplorasi Uranium Eko Remaja, Kalan, Kalimantan Barat," *Eksplorium*, vol. 37, no. 2, pp. 89–100, 2016.

[3] Ngadenin, "Recent Activities in the Uranium Mining Tunnel, West Kalimantan, Indonesia," 2019. [Online]. Available: https://nucleus.iaea.org/sites/connect/UPCpublic/UMREG Presentations/Indonesia_Recent Activities in The Uranium Mining Tunnel%2C West Kalimantan.pdf.

[4] Y. Faizah, W. Cakrabuana, D. Kamajati, and P. Rahmawati, "Analisis Kualitas dan Perkuatan Massa Batuan Terowongan Eksplorasi Uranium Eko Remaja Kalan, Kalimantan Barat Menggunakan Metode RMR (Rock Mass Rating)," *Eksplorium*, vol. 41, no. 1, pp. 25–36, May 2020, doi: https://www.doi.org/10.17146/eksplorium.2020.41.1.5859.

[5] H. Syaeful, I. G. Sukadana, Y. S. B. Susilo, F. D. Indrastomo, A. G. Muhammad, and Ngadenin, "Uranium Exploration, Deposit and Resources: The Key of Nuclear Power Plant Development Program in Indonesia," in *Journal of Physics: Conference Series*, Yogyakarta: IOP Publishing, 2021. doi: https://www.doi.org/10.1088/1742-6596/2048/1/012003.

[6] H. Farhadian, H. Katibeh, P. Huggenberger, and C. Butscher, "Optimum model extent for numerical simulation of tunnel inflow in fractured rock," *Tunn. Undergr. Sp. Technol.*, vol. 60, pp. 21–29, 2016, doi: https://www.doi.org/10.1016/j.tust.2016.07.014.

[7] H. Syaeful and Suharji, "Geostatistics Application on Uranium Resources Classification: Case Study of Rabau Hulu Sector, Kalan, West Kalimantan," *Eksplorium*, vol. 39, no. 2, pp. 131–140, 2018, doi: https://www.doi.org/10.17146/eksplorium.2018.39.2.4960.

[8] A. M. Sharaky, K. M. A. El Maksoud, F. Oraby, H. M. Haridy, H. I. El Sundoly, and M. S. A. El Azim, "Practical Estimates of Rock Mass Strength and Deformation Modulus: A Case Study of Gattar-V Uranium Occurrence, Arabo-African Shield," *Iraqi Natl. J. Earth Sci.*, vol. 25, no. 2, pp. 320–330, 2025, doi: https://www.doi.org/10.33899/earth.2024.145626.1203.

[9] C. Morrish, "Mining Techniques for Uranium Ore Pod Recovery," McGill University, 1997.

[10] Norwegian Geotechnical Institute, *Using the Q-system - Rock mass classification and support design*. Oslo: Norwegian Geotechnical Institute, 2025.

[11] P. R. Joshi, M. Kharel, A. Poudel, G. R. Joshi, and D. Sapkota, "Correlation of Rock Mass Rating (RMR), Tunneling Quality Index (Q), and Geological Strength Index (GSI) in Pre-Cambrian Dolomite Based on Field Data," in *4th European Regional Conference of IAEG*, Dubrovnik: IAEG, 2024, pp. 11–23. doi: https://www.doi.org/10.5592/CO/EUROENGEO.2024.105.

[12] H. Rehman, W. Ali, A. M. Naji, J. Kim, R. A. Abdullah, and H. Yoo, "Review of Rock-Mass Rating and Tunneling Quality Index Systems for Tunnel Design: Development, Refinement, Application and Limitation," *Appl. Sci.*, vol. 8, no. 8, p. 1250, 2018, doi: https://www.doi.org/10.3390/app8081250.

[13] R. Ulusay and J. A. Hudson, *The complete ISRM suggested methods for rock characterization, testing and monitoring: 1974-2006*. Ankara: The ISRM Turkish National Group, 2007. [Online]. Available: https://www.scirp.org/reference/referencespapers?referenceid=1673351.

[14] H. I. Chaminé, M. J. Afonso, L. Ramos, and R. Pinheiro, "Scanline Sampling Techniques for Rock Engineering Surveys: Insights from Intrinsic

Geologic Variability and Uncertainty," in *Engineering Geology for Society and Territory*, Springer, 2015, pp. 357–361. doi: https://www.doi.org/10.1007/978-3-319-09060-3_61.

[15] W. Ali, R. A. Abdullah, H. Rehman, and M. Junaid, "The effect of scanline direction and extent of rock exposure on assessment of geometrical properties of discontinuities in rock mass," in *IOP Conference Series: Materials Science and Engineering*, Kuala Lumpur: IOP Publishing, 2019. doi: https://www.doi.org/10.1088/1757-899X/527/1/012034.

[16] B. Lepillier P-O. Bruna, D. Bruhn, E. Bastesen, A. Daniilidis, Ó. Garcia, A. Torabi, and W. Wheeler, "From outcrop scanlines to discrete fracture networks, an integrative workflow," *J. Struct. Geol.*, vol. 133, no. 103992, 2020, doi: https://www.doi.org/10.1016/j.jsg.2020.103992.

[17] C. Zangerl, M. Koppensteiner, and T. Strauhal, "Semiautomated Statistical Discontinuity Analyses from Scanline and Other Methods," *Appl. Sci.*, vol. 12, no. 19, 2022, doi: https://www.doi.org/10.3390/app12199622.

[18] N. Barton, R. Lien, and J. Lunde, "Engineering classification of rock masses for the design of tunnel support," *Rock Mech. Rock Eng.*, vol. 6, no. 4, pp. 189–236, 1974, doi: https://www.doi.org/10.1007/BF01239496.

[19] E. Grimstad and N. Barton, "Updating of the Q-system for NMT," in *International Symposium on Sprayed Concrete*, Fagernes, 1993, pp. 46–66. [Online]. Available: https://www.scirp.org/reference/referencespapers?referenceid=2013391.

[20] H. S. Karyono, "Analisis Kontrol Tektonik pada Vein Mineralisasi di Bukit Eko, Kalan, Kalimantan Barat," in *Prosiding PIT IAGI*, 1991, pp. 115–128.

[21] R. Sahputra, "Identification of Radiometric and Mineragraphy Analysis of Uranium and Sulfide Mineral at BM-179 Kalan-West Kalimantan Uranium Ore," *Am. Sci. Res. J. Eng. Technol. Sci.*, vol. 14, no. 2, pp. 311–321, 2015, [Online]. Available: https://asrjetsjournal.org/American_Scientific_Journal/article/view/1062.

[22] A. G. Muhammad, R. C. Ciputra, and H. Syaeful, "Fracture Analysis of Uranium-Bearing Rock in Eko-Remaja Exploration Tunnel at Depth 50-200 Meters, Kalan, West Kalimantan," in *Journal of Physics: Conference Series*, IOP Publishing, 2019. doi: https://www.doi.org/10.1088/1742-6596/1363/1/012013.

[23] R. C. Ciputra, M. N. Heriawan, H. Syaeful, D. Kamajati, and P. Rahmawati, "Geostatistical Ore Body Modeling on Uranium Mineralization in Remaja Sector, Kalan Area, West Kalimantan," *Eksplorium*, vol. 43, no. 1, pp. 41–58, 2022, doi: https://www.doi.org/10.17146/eksplorium.2022.43.1.6622.

[24] Amiruddin and D. S. Trail, *Peta Geologi Lembar Nanga Pinoh, Kalimantan*. Bandung, 1993.

[25] W. Cakrabuana, E. N. S. Argianto, R. C. Ciputra, and D. Kamajati, "Geological, Geochemical, and Radiometric Study of Sandstone-type Uranium Deposit Exploration in Menukung Area, West Borneo," *IAGI J.*, vol. 1, no. 1, pp. 1–12, 2021, doi: https://www.doi.org/10.51835/iagij.2021.1.1.15.

[26] B. Batara and C. Xu, "Evolved magmatic arcs of South Borneo: Insights into Cretaceous slab subduction," *Gondwana Res.*, vol. 111, pp. 142–164, 2022, doi: https://www.doi.org/10.1016/j.gr.2022.08.001.

[27] R. A. Farrenzo, R. D. Nugraheni, I. G. Sukadana, F. D. Indrastomo, and T. B. Adimedha, "Characterization of Metapelite and Metasiltstone as Uranium-REE hosted rocks in Rirang Area, West Kalimantan," in *IOP Conference Series: Earth and Environmental Science*, IOP Publishing, 2023. doi: https://www.doi.org/10.1088/1755-1315/1233/1/012027.

[28] F. D. Indrastomo, I. G. Sukadana, T. B. Adimedha, W. Cakrabuana, R. Fauzi, H. Syaeful, R. C. Ciputra, and Y. Rachael, "Uranium Deposit Reflection from Radon-Thoron in Melawi Basin, West Kalimantan," in *International Conference on Nuclear Science, Technology, and Applications – ICONSTA 2022*, Tangerang Selatan: AIP Publishing, 2024, p. 9. doi: https://www.doi.org/10.1063/5.0192880.

[29] S. Tjokrokardono, B. Soetopo, L. Subiantoro, and K. S. Widana, "Geologi dan Mineralisasi Uranium Kalan, Kalimantan Barat," in *Laporan Hasil Penelitian Tahun 2005*, Jakarta: Batan, 2005, pp. 27–52.

[30] H. T. Breitfeld, L. Davies, R. Hall, R. Armstrong, M. Forster, G. Lister, M. Thirlwall, N. Grassineau, J. H. Breitfeld, and M. W. A. van Hattum, "Mesozoic Paleo-Pacific Subduction Beneath SW Borneo: U-Pb Geochronology of the Schwaner Granitoids and the Pinoh Metamorphic Group," *Front. Earth Sci.*, vol. 8, pp. 1–37, 2020, doi: https://www.doi.org/10.3389/feart.2020.568715.

[31] R. C. Ciputra, Suharji, D. Kamajati, and H. Syaeful, "Application of geostatistics to complete uranium resources estimation of Rabau Hulu Sector, Kalan, West Kalimantan," in *E3S Web of Conferences*, E3S, 2020. doi: https://www.doi.org/10.1051/e3sconf/202020006001.

[32] L. Davies, R. Hall, and M. Forster, "Age and Character of Basement Rocks in SW Borneo — Ar-Ar dating of Pinoh Metamorphic Group rocks," in *Tectonic Evolution and Sedimentation of South China Sea Region*, Kinabalu: AAPG, 2015. [Online]. Available: https://www.searchanddiscovery.com/pdfz/abstra

p-ISSN 0854-1418
e-ISSN 2503-426X

cts/pdf/2015/90236apr/abstracts/ndx_davies.pdf.html.

[33] X. Qian, Y. Yu, Y. Wang, C. Gan, Y. Zhang, and J. B. Asis, "Late Cretaceous Nature of SW Borneo and Paleo-Pacific Subduction: New Insights from the Granitoids in the Schwaner Mountains," *Lithosphere*, vol. 1, pp. 1–22, 2022, doi: https://www.doi.org/10.2113/2022/8483732.

[34] Y. Wang, S. Wu, X. Qian, P. A. Cawood, X. Lu, C. Gan, J. Bin Asis, and P.Zhang, "Early Cretaceous subduction in NW Kalimantan: Geochronological and geochemical constraints from the Raya and Mensibau igneous rocks," *Gondwana Res.*, vol. 101, pp. 243–256, 2022, doi: https://www.doi.org/10.1016/j.gr.2021.08.006.

[35] P. R. Williams, C. R. Johnston, R. A. Almond, and W. H. Simamora, "Late Cretaceous to Early Tertiary Structure Element of West Kalimantan," in *Tectonophysics*, 1988, pp. 279–297. doi: https://www.doi.org/10.1016/0040-1951(88)90135-7.

[36] H. S. Karyono and M. Ruhland, "Use of multiscalar processing of remotely sensed data in Kalan fracturation networks, west Kalimantan, Indonesia, for future mineralisations research," *ISPRS J. Photogramm. Remote Sens.*, vol. 45, no. 5–6, pp. 428–441, 1990, doi: https://www.doi.org/10.1016/0924-2716(90)90033-8.

[37] A. G. Muhammad and F. D. Indrastomo, "Validitas dan Reliabilitas Data Estimasi Kadar Uranium Sektor Lembah Hitam, Kalan, Kalimantan Barat," *Eksplorium*, vol. 40, no. 2, pp. 75–88, 2019, doi: https://www.doi.org/10.17146/eksplorium.2019.40.2.5672.

[38] T. B. Adimedha, R. A. Farrenzo, I. G. Sukadana, R. D. Nugraheni, F. Pratiwi, R. C. Ciputra, F. D. Indrastomo, H. Syaeful, and Y. Rachael, "Distribution and Characteristics of Rare Earth Elements in Uranium-Ore Deposits from Rirang Area, West Kalimantan Province, Indonesia," *Eksplorium*, vol. 45, no. 1, pp. 1–16, 2024, doi: https://www.doi.org/10.55981/eksplorium.2024.7058.

[39] J. A. Hudson, *Rock Mechanics Principles in Engineering Practice*. London: CIRIA/Butterworths, 1989.

[40] N. Kumar, "Rock mass characterisation and evaluation of supports for tunnels in Himalaya," Indian Institute of Technology Roorkee, 2002. [Online]. Available: http://hdl.handle.net/123456789/6714.

[41] H. Rehman, A. M. Naji, J. Kim, and H. Yoo, "Empirical Evaluation of Rock Mass Rating and Tunneling Quality Index System for Tunnel Support Design," *Appl. Sci.*, vol. 8, no. 5, p. 782, 2018, doi: https://www.doi.org/10.3390/app8050782.

[42] J. Lee, H. Rehman, A. M. Naji, J. Kim, and H. Yoo, "An Empirical Approach for Tunnel Support Design through Q and RMi Systems in Fractured Rock Mass," *Appl. Sci.*, vol. 8, no. 12, p. 2659, 2018, doi: https://www.doi.org/10.3390/app8122659.

[43] D. U. Deere, "Technical Description of Rock Cores for Engineering Purposes," *Rock Mech. Eng. Geol.*, vol. 1, no. 1, pp. 16–22, 1963.

[44] S. D. Priest and J. A. Hudson, "Discontinuity spacings in rock," *Int. J. Rock Mech. Min. Sci.*, vol. 13, no. 5, pp. 135–148, 1976, doi: https://www.doi.org/10.1016/0148-9062(76)90818-4.

[45] N. Barton, "Some new Q-value correlations to assist in site characterisation and tunnel design," *Int. J. Rock Mech. Min. Sci.*, vol. 39, no. 2, pp. 185–216, 2002, doi: https://www.doi.org/10.1016/S1365-1609(02)00011-4.

[46] N. Barton, "Training course on rock engineering," New Delhi, 2008.

[47] E. Grimstad, K. Kankes, R. Bhasin, A. Magnussen, and A. Kaynia, "Rock mass quality Q used in designing reinforced ribs of sprayed concrete and energy absorption," in *International Symposium on Sprayed Concrete*, Davos: Norwegian Geotechnical Institute, 2002, pp. 134–142. [Online]. Available: https://www.semanticscholar.org/paper/ROCK-MASS-QUALITY-Q-USED-IN-DESIGNING-REINFORCED-OF-Grimstad-Kankes/156bbd10ea2b538c151dbde23a40a4af4dcbb0f9.

[48] Rocscience, *RocLab 1.0 - Rock mass strength analysis using the generalized Hoek-Brown failure criterion*. Rocscience, 2007. [Online]. Available: https://www.resolutionmineeis.us/sites/default/files/references/rocscience-2007.pdf.

[49] E. Hoek, C. Carranza-Torres, and B. Corkum, "Hoek-Brown Failure Criterion - 2002," in *North American Rock Mechanics Symposium*, Toronto: Tunnel Association of Canada, 2002, pp. 267–273. [Online]. Available: https://www.rocscience.com/assets/resources/learning/hoek/Hoek-Brown-Failure-Criterion-2002.pdf.

[50] R. E. Aufmuth, "A systematic determination of engineering criteria for rocks," *Eng. Geol.*, vol. 11, pp. 235–245, 1973, doi: https://www.doi.org/10.1016/0148-9062%2875%2990749-4.

[51] E. Hoek, T. G. Carter, and M. S. Diederichs, "Quantification of the Geological Strength Index Chart," in *47th US Rock Mechanics/Geomechanics Symposium*, San Fransisco: ARMA, 2013, pp. 1757–1764. [Online]. Available: https://www.rocscience.com/assets/resources/lear

ning/hoek/2013-Quantification-of-the-GSI-Chart.pdf.

[52] P. Marinos and E. Hoek, "A geologically friendly tool for rock mass strength estimation," in *ISRM International Symposium*, Melbourne: ISRM, 2000. [Online]. Available: https://www.rocscience.com/assets/resources/learning/hoek/2000-GSI-A-Geologically-Friendly-Tool-for-Rock-Mass-Strength-Estimation.pdf.

[53] E. Hoek, *Practical Rock Engineering*. British Columbia: Rocscience, 2007. [Online]. Available: https://www.rocscience.com/hoek/corner/Practical_Rock_Engineering.pdf.

[54] H. Syaeful and D. Kamajati, "Analisis Karakteristik Massa Batuan di Sektor Lemajung, Kalan, Kalimantan Barat," *Eksplorium*, vol. 36, no. 1, pp. 17–30, 2015, doi: https://www.doi.org/10.17146/eksplorium.2015.36.1.2768.